



TECHNICAL UNIVERSITY OF CLUJ-NAPOCA

ACTA TECHNICA NAPOCENSIS

Series: Applied Mathematics and Mechanics
Vol. 55, Issue III, 2012

INVERSE DYNAMIC MODEL OF A NEW PARALLEL ROBOT USED IN MINIMALLY INVASIVE SURGERY

Alin STOICA, Bogdan GHERMAN, Calin VAIDA, Doina PISLA, Nicolae PLITEA

Abstract: Due to robotic assisted surgery the surgeons can operate through infinitely smaller incisions, resulting some benefits for the patients, like: less trauma, reduced blood loss, shorter recovery time, as well as for doctors, providing benefits such as reduction in hand tremor, 3D visualization and workspace scaling. Using the principle of virtual work, the inverse dynamic model of a new parallel architecture is determined and some simulation results are presented in this paper. **Key words:** parallel robot, inverse dynamic model, minimally invasive surgery, simulation results.

1. INTRODUCTION

Minimally invasive surgery (MIS) has evolved and developed continuously in the last 20 years. This procedure typically involves the use of several small sized incisions to introduce an endoscope together with the surgical instruments which provides an indirect view of the surgical field. In a MIS procedure, some of the demonstrated patient advantages are: less trauma, reduced blood loss, shorter recovery time, less emotional discomfort, less morbidity. Robots are useful tools in minimally invasive surgery (MIS), providing benefits such as reduction in hand tremor, navigation, and workspace scaling.

The first surgical robotic application for positioning the laparoscopic camera within the surgical field was performed, in 1993 with the help of AESOP 1000 robotic system [1]. Prosurgrics provides FreeHand [2], a robotic system that positions the laparoscopic camera based on the head motions of the surgeon. Another surgical robot is ViKY developed by EndoControl [3], [4], which is a compact motorized endoscope holder for a wide range of laparoscopic and thoracic surgeries. One of the most complex surgical robots used in MIS is the da Vinci surgical system [5] developed in 1997 by Intuitive Surgical Inc. and

currently at the second generation, approved for medical use, namely in surgery and urology.

The first steps in this field of research in Romania were achieved at the Technical University of Cluj-Napoca in 2005, and the first experimental model of a laparoscopic holder with 3 DOF, named PARAMIS was achieved in 2008 [6, 7]. PARASURG 5M is another system [8] designed for minimally invasive surgery, developed at the Technical University of Cluj-Napoca.

The dynamic analysis of parallel structures has an important role in the description of the behaviour of mechanical systems and in the achievement of their best performances. The inverse dynamics aims to describe and to find the actuator forces and/or torques needed to generate a desired trajectory of the end-effector (surgical instrument or laparoscope).

The principle of virtual work will be applied in this paper. Constraint forces and torques, depending on the choice of system coordinates, may also be taken into consideration. The principle of virtual work is the most efficient method for the dynamic analysis of parallel manipulators [9]. Different researchers [10, 11] present the dynamic analysis of parallel manipulators based on this principle. The dynamic

modeling and a control for a three prismatic revolute cylindrical parallel kinematic machine using the principle of virtual work is described in [12]. The kinematic and dynamic analysis of a 4-DOF parallel manipulator using the principle of virtual power, presenting the recursive matrix equations is presented in [13]. Itul and Pisla present a comparative study between different dynamical methods for 3 DOF parallel robots considering certain parameters [14, 15]. Seyferth [16] proves that the minimum number of lumped masses that can dynamically replace a rigid body correct is four. Sixteen parameters m_i, x_i, y_i, z_i ($i = 1, 2, 3, 4$) characterize the mass replacement procedure, six of them may be chosen freely. In case the rigid body forms a bar of length $l_i = l$ with longitudinally and evenly distributed mass $m_i = m$, the system is dynamically equivalent to three masses: $m_1 = m_2 = m/6$, $m_3 = 2m/3$ [17], the mass m_3 being located in the bar centre of the mass and the other two masses at the end points of the bar.

2. INVERSE DYNAMIC MODEL

Starting from the parallel structure presented in [18] and [8], a new parallel module for orientation is attached to the structure described in [19]. This new parallel structure reduces the pressure on the abdominal wall and can handle both a laparoscope and an active instrument for different operations such as cutting, suturing, grasping. The advantage of this new parallel structure from the kinematic point of view is that its both direct and inverse geometric models have been obtained through an analytical approach.

The implicit equations defining the tip of the endoscope are:

$$\begin{cases} f_1(q_1, q_2, q_3, X_G, \psi, \theta) \equiv X_G - h \cdot \cos(\psi) \cdot \sin(\theta) \\ -(\sqrt{(2 \cdot b)^2 - (q_2 - q_1)^2} \cdot \cos(q_3) - 1 \cdot \sin(\beta) \cdot \cos(q_3)) = 0 \\ f_2(q_1, q_2, q_3, Y_G, \psi, \theta) \equiv Y_G - h \cdot \sin(\psi) \cdot \sin(\theta) \\ -(\sqrt{(2 \cdot b)^2 - (q_2 - q_1)^2} \cdot \sin(q_3) - 1 \cdot \sin(\beta) \cdot \sin(q_3)) = 0 \\ f_3(q_1, Z_G, \theta) \equiv Z_G + h \cdot \cos(\theta) - (q_1 - 1 \cdot \cos(\beta)) = 0 \\ f_4(q_1, q_2, q_3, q_4, q_5, \psi, \theta) \equiv -\sin(\theta) \cdot \cos(\psi - q_3) - \sin(q_4) = 0 \\ f_5(q_3, q_5, \psi, \theta) \equiv \sin(\psi - q_3) \cdot \sin(\beta + q_4) - \sin(q_5) = 0 \end{cases}$$

(1)

Using the matrix representation, the kinematic model is:

$$A \cdot \dot{X} + B \cdot \dot{q} = 0 \tag{2}$$

In the case of **inverse kinematic model**, the end-effector velocities $\dot{X} = [\dot{X}_G \ \dot{Y}_G \ \dot{Z}_G \ \dot{\psi} \ \dot{\theta}]^T$ and end-effector acceleration $\ddot{X} = [\ddot{X}_G \ \ddot{Y}_G \ \ddot{Z}_G \ \ddot{\psi} \ \ddot{\theta}]^T$ are given, while the driving velocities and accelerations $\dot{q} = [\dot{q}_1 \ \dot{q}_2 \ \dot{q}_3 \ \dot{q}_4 \ \dot{q}_5]^T$, $\ddot{q} = [\ddot{q}_1 \ \ddot{q}_2 \ \ddot{q}_3 \ \ddot{q}_4 \ \ddot{q}_5]^T$ are computed.

$$\dot{q} = -B^{-1} \cdot A \cdot \dot{X} \tag{3}$$

$$\ddot{q} = -B^{-1} \cdot (\dot{A} \cdot \dot{X} + A \cdot \ddot{X} + \dot{B} \cdot \dot{q}) \tag{4}$$

The inputs for the generation of the equations of the **inverse dynamic model** are: the motion laws of the robot on the end-effector coordinates, the inverse kinematic model and the masses of robot elements. The outputs are the drive forces/torques. The principle of virtual work is applied in order to get these drive forces/torques. The torque vector is:

$$\tau = [\tau_1, \tau_2, \tau_3, \tau_4, \tau_5]^T = [F_1, F_2, M_3, M_4, M_5]^T \tag{5}$$

Figure 1 presents the structure of the robot, indicating the main mechanical elements that are considered.

The inverse dynamics is determined for the case in which the robot is used as a laparoscope holder, so there will be no tissue contact between the tip of the endoscope and the internal organs. The friction forces in all joints have been also neglected.

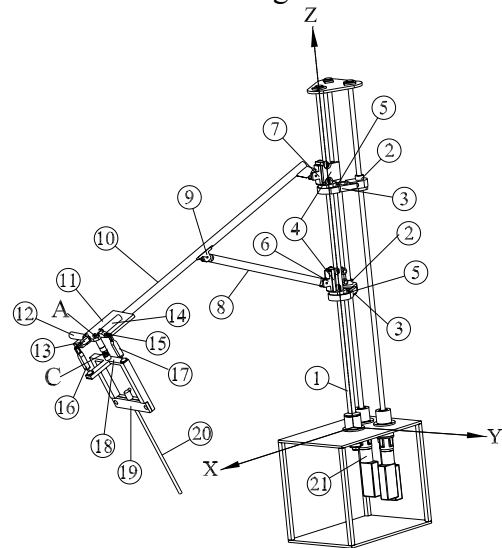


Fig. 1. The parallel structure

The following elements are considered:

- the central column (1) having the mass m_1 , consisting of the central shaft of mass m_{arb} and the driven pulley with mass m_r ;
- the screw nuts (two pieces) - (2) each one with mass m_2 , and the connecting pieces between them and the central shaft (3) with the mass m_3 ;
- the components (bearing and other connecting pieces) which build up the upper and the lower sliding carriage (running on the central shaft), each noted with (4) have the mass m_4 ;
- the bearings ensuring the rotation of the shaft around the connecting pieces between the screw nuts and the shaft, noted with (5), have the mass m_5 ;
- the coupling element of the lower rod (8) with the mass m_8 , and lower sliding carriage, noted with (6), have the mass m_6 ;
- the coupling element of the upper rod (10) with mass m_{10} , and the upper sliding carriage, noted with (7), have the mass m_7 ;
- the lower rod (8) with mass m_8 ;
- the coupling element of the two rods (9) with mass m_9 ;
- the upper rod (10) with mass m_{10} ;
- the fixed platform of the parallel module (11) with mass m_{11} ;
- the motor (actuator) and the speed reducer as well the fixing element corresponding to the active joint q_4 noted with (12) of mass m_{12} ;
- the active joint q_4 noted with (13) of mass m_{13} ;
- the motor (actuator) and the speed reducer as well the fixing element corresponding to the active joint q_5 noted with (14) of mass m_{14} ;
- the active joint q_5 noted with (15) of mass m_{15} ;
- the passive joint driven by the active joint q_4 noted with (16) of mass m_{16} ;
- the passive joint driven by the active joint q_5 noted with (17) of mass m_{17} ;
- the mobile platform of the parallel module, where will attach laparoscope and the active instrument, noted with (18) of mass m_{18} ;

- the piece that locks the laparoscope noted with (19) of mass m_{19} ;
- the laparoscope, noted with (20) and having the mass m_{20} ;
- the actuator which ensures the rotation to the active joint q_3 is noted with (21) of mass m_{21} ;

The elements of length are l_i , $i = 1..18$.

Starting from the principle of lumped masses, 33 equivalent masses have been obtained, their distribution being described in figure 2.

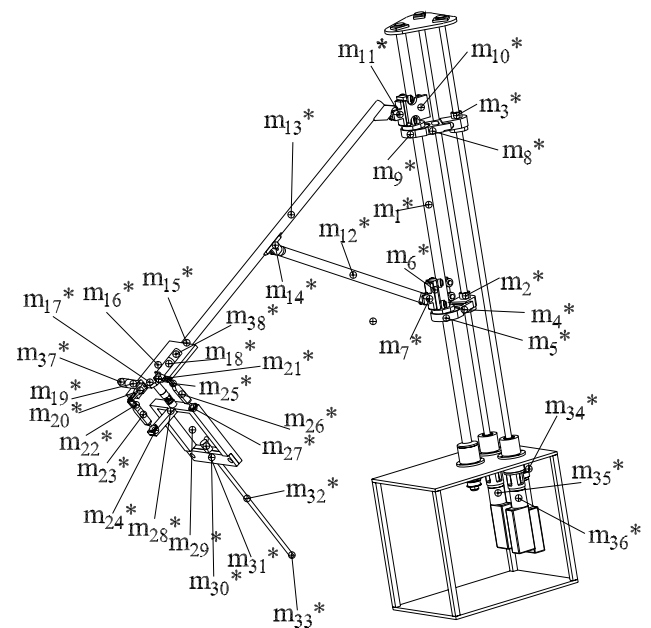


Fig. 2. The parallel robot with mass distribution

m_i^* are the lumped masses of the robot elements and joints having the masses m_i , $i = 1, 2, \dots, 36$ and coordinates X_i, Y_i, Z_i , $i = 1, 2, \dots, 36$;

One can see that:

$$\begin{cases} X_G = X_{33}, \\ Y_G = Y_{33}, \\ Z_G = Z_{33}, \end{cases} \quad (6)$$

The influence of the relative motion of the elements, involved in a rotation motion is computed for the two active joints of the actuating the ball screw (2), for the motor (21) and the motors (12) and (14).

The moments of inertia of the motor and speed reducer have been obtained from the catalogues: I_{mot} , I_r .

The moment of inertia for the screw [18] is:

$$I_A = (m_s \cdot D^2) / (8 \cdot 10^6) \text{ [kg} \cdot \text{m}^2] \quad (7)$$

where m_s is the screw mass, and D is the diameter of the screw.

The moment of inertia for the motor-speed reducer-screw clutch [20] is:

$$I_B = (m_c \cdot D_1^2) / (8 \cdot 10^6) \text{ [kg} \cdot \text{m}^2] \quad (8)$$

where m_c is the mass of the clutch and D_1 is the diameter of the clutch.

The reduced moment of inertia could be determined by the relation:

$$I_{red} \cdot \dot{\varphi}_1^2 / 2 = I_{mot} \cdot (\dot{\varphi}_1 \cdot n_1)^2 / 2 + \dot{\varphi}_1^2 / 2 \cdot (I_r + I_A + I_B) \quad (9)$$

$$I_{red34} = I_{red35} = I_{mot} \cdot n_1^2 + I_r + I_A + I_B \quad (10)$$

where n_1 is gear ratio between the motor q_1 and his speed reducer.

The coordinates of the mass 34 are:

$$X_{34} = i_{\Delta34} \cdot \cos(\varphi_1); \quad Y_{34} = i_{\Delta34} \cdot \sin(\varphi_1); \quad Z_{34} = -l_2 \quad (11)$$

where:

$$i_{\Delta34} = i_{\Delta35} = \sqrt{I_{red} / m_{tot}} \quad (12)$$

knowing that:

$$m_{34}^* = m_{35}^* = m_{tot} = m_s + m_r + m_m + m_c \quad (13)$$

m_r and m_m are the masses in rotation of the speed reducer and motor, and:

$$\varphi_1 = \varphi_{10} + (2\pi) / P \cdot (q_1 - q_{10}) \quad (14)$$

where q_{10} represents the position of the motor 1 at the beginning of motion and φ_{10} is the initial value of the rotation angle the point "34" has with respect to Z axis.

For the active joint q_2 :

$$X_{35} = i_{\Delta35} \cdot \cos(\varphi_2); \quad Y_{35} = i_{\Delta35} \cdot \sin(\varphi_2); \quad Z_{35} = -l_2 \quad (15)$$

where:

$$\varphi_2 = \varphi_{20} + (2\pi) / P \cdot (q_2 - q_{20}) \quad (16)$$

Taking into account that the motor and speed reducer are identical with the first joints, I_{mot} , I_r can be used.

If D_2 is the contact diameter of the driven pulley:

$$I_{RC} = (m_{rc} \cdot D_2^2) / (8 \cdot 10^6) \text{ [kg} \cdot \text{m}^2] \quad (17)$$

This represents the moment of inertia of the driven pulley mounted on the motor.

q_3 is obtained at the speed reducer output, the relation is:

$$I_{red21} \cdot \dot{q}_3^2 / 2 = I_r \cdot \dot{q}_3^2 / 2 + I_{mot} \cdot (n_2 \cdot \dot{q}_3)^2 / 2 + I_{RC} \quad (18)$$

where n_2 is the gear ration between the motor and speed reduction unit.

Thus:

$$I_{red21} = I_r + I_{mot} \cdot n_2^2 + I_{RC} \quad (19)$$

The lumped mass 36 is:

$$m_{36}^* = m_{red21} = m_r + m_{mot} \quad (20)$$

The position of the dynamic equivalent mass point is determined by the gyration radius:

$$i_{\Delta36} = \sqrt{I_{red21} / m_{red21}} \quad (21)$$

$$X_{36} = i_{\Delta36} \cdot \cos(q_3); \quad Y_{36} = i_{\Delta36} \cdot \sin(q_3); \quad Z_{36} = -l_1 \quad (22)$$

The moments of inertia of the motor and speed reducer are considered only for the active joints (12) and (14). The values can be taken from the manufacturer's catalogue: I_{r_or} and I_{m_or} . It yields:

$$I_{red12} = I_{red14} = I_{r_or} + I_{m_or} \cdot n_3^2 \quad (23)$$

where n_3 represents the gear ratio between the motor and speed reduction unit.

The equivalent mass 37 is:

$$m_{37}^* = m_{38}^* = m_{red12} = m_{red14} = m_{r_or} + m_{m_or} \quad (24)$$

The position of the equivalent mass point (37) is determined by the gyration radius:

$$i_{\Delta37} = \sqrt{I_{red12} / m_{red12}} \quad (25)$$

$$\begin{cases} X_{37} = i_{\Delta37} \cdot \cos(q_4) + X_A + l_5 \cdot \sin(q_3); \\ Y_{37} = i_{\Delta37} \cdot \sin(q_4) + Y_A - l_5 \cdot \cos(q_3); \\ Z_{37} = q_1 \end{cases} \quad (26)$$

The position of the mass point (38) is determined by the gyration radius:

$$i_{\Delta38} = \sqrt{I_{red14} / m_{red14}} \quad (27)$$

$$\begin{cases} X_{38} = i_{\Delta31} \cdot \cos(q_5) + X_A - l_7 \cdot \cos(q_3); \\ Y_{38} = i_{\Delta31} \cdot \sin(q_5) + Y_A - l_7 \cdot \sin(q_3); \\ Z_{38} = q_1 \end{cases} \quad (28)$$

The virtual work principle was used in order to obtain the dynamic model of the parallel robot. It has the following form:

$$\delta W = \delta q^T \cdot \tau + \sum_{i=1}^{38} \delta X_{Mi}^T \cdot (T_i^{Tr} + T_i^g) = 0 \quad (29)$$

The coordinates of M_i points can be determined with respect to the coordinates of the active joints (in the same way as these

coordinates represent the end-effector coordinates), obtaining the relations:

$$\delta X_{M_i} = J_i \cdot \delta q \quad (30)$$

$$\delta X_{M_i}^T = \delta q^T \cdot J_i^T \quad (31)$$

From (25) the torque vector is obtained:

$$\tau = -\sum_{i=0}^{38} J_i^T \cdot (T_i^{Tr} + T_i^g) \quad (32)$$

2. SIMULATION RESULTS

Some simulations of the end-effector motions were achieved based on the inverse dynamic model of the parallel robot.

Considering all these parameters, a trajectory of the tip of the laparoscope has been imposed (meaning the initial and final position of the laparoscope). This trajectory is inside the abdominal cavity of the patient within the robot workspace, as in a real displacement of the laparoscope, when the surgeon inspects the operating field.

The trajectory is **linear in space** and similar to a real one, as the instrument is controlled by the joystick, when the surgeon wants to focus the camera in the robot workspace.

The simulation results for the inverse dynamic model of parallel robot for a linear trajectory are showed in the figure 3.

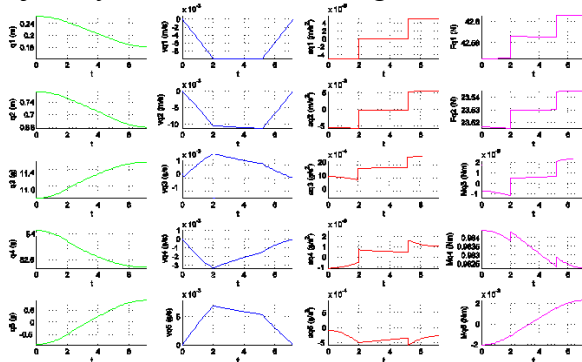


Fig. 3. Simulation results for the inverse dynamic model of parallel robot for a linear trajectory between two points in space

4. CONCLUSION

In this paper the inverse dynamic model of the parallel robot used in MIS has been presented. Starting from mass geometry considerations, which consists in replacing correctly a given multibody system by

dynamically equivalent single masses, the method of virtual work is proposed. The advantage of this new approach consists in obtaining the inverse dynamic model in an analytical way. Based on the principle of virtual work, this method proves to be more efficient as it can eliminate all forces and internal joints allowing direct determination of forces/torques of the robot for the given laws of motion of the end effector. The use of this approach shows that the dynamic model of the robot can be computed with simple and fast computing equations. Some simulation results based on the inverse dynamics are also presented.

ACKNOWLEDGEMENTS

This paper was supported by the projects "Doctoral studies in engineering sciences for developing the knowledge based society-SIDOC" contract no. POSDRU/88/1.5/S/60078 co-funded from European Social Fund through Sectorial Operational Program Human Resources 2007-2013 and Scopes International Grant IZ74Z0-137361 entitled "Creative Alliance in Research and Education focused on Medical and Service Robotics (CARE-Robotics)".

5. REFERENCES

- [1] Brown University, Division of Biology and Medicine, <http://biomed.brown.edu>
- [2] P.A. Finlay, "A New Miniature Manipulator for Laparoscopic Camera Control", WC on Medical Physics and Biomedical Eng., Germany, DOI 10.1007/978-3-642-03906-5-34, 2009.
- [3] A. Gumbs, et. al., "Totally Transumbilical Laparoscopic Cholecystectomy", in J. Gastrointest Surg 13:533-534, DOI 10.1007/s1105-008-0614-8, 2009.
- [4] S. Voros, et. al., "ViKY Robotic Scope Holder: Initial Clinical Experience and Preliminary Results Using Instrument Tracking", IEEE/ASME Transactions on Mechatronics, 2010, Vol. 15, Issue 6, pp. 879 - 886, 2010.
- [5] <http://www.riverviewregional.com/>
- [6] D. Pisla, N. Plitea, C. Vaida, "Kinematic Modeling and Workspace Generation for a New Parallel Robot Used in Minimally Invasive Surgery". In Advances in Robot Kinematics, DOI 10.1007/978-1-4020-8600-7_48, 2008.

- [7] C. Vaida, D. Pislă, N. Plitea, B. Gherman, et.al, "Development of a Control System for a Parallel Robot used in Minimally Invasive Surgery", Meditech 2009, in IFMBE Proceedings Series, ISSN 1680-0737, 2009.
- [8] B. Gherman, D. Pislă, (corresponding author), C. Vaida, N. Plitea, *Development of Inverse Dynamic Model for a Surgical Hybrid Parallel Robot with Equivalent Lumped Masses*, Robotics and Computer-Integrated Manufacturing, 2011, doi:10.1016/j.rcim.2011.11.003.
- [9] L.W. Tsai, *Robot Analysis: The Mechanics of Serial and Parallel Manipulators*. Wiley, New York, 1999.
- [10] S. Staicu, D.C Carp-Ciocordia: *Dynamic analysis of Clavel's delta parallel robot*. In: Proc. IEEE Int. Conf. Robot. Autom., vol. 3, pp. 4116–4121, 2003.
- [11] W. Khalil, O. Ibrahim: *General solution for the dynamic modeling of parallel robots*. In: Proc. IEEE Int. Conf. Robot. Autom., vol. 4, pp. 3665–3670, 2004.
- [12] Li Y, Xu Q, *Dynamic modeling and robust control of a 3-PRC translational parallel kinematic machine*, J Robotics Computer-Integrated Manufacturing. 25-3, 630-640, 2009.
- [13] S. Staicu, D. Zhang, *Dynamic modelling of a 4-DOF parallel kinematic machine with revolute actuators*. Int. J Manufact. 3, 172–187, 2008.
- [14] S. Staicu, *Recursive Modelling in Dynamics of Delta parallel robot*, Robotica. An International Journal 27, 199-207, 2009.
- [15] T. Itul, D. Pislă, *Comparative Study between D'Alembert Principle and Lagrange Formulation for Guiding in three Points Parallel Robot Dynamic Analysis*, In Proc. of 14 th International Conference on Control Systems and Computer Science, Politehnica Press, Bucharest 1, 100-105, 2003.
- [16] W. Seyferth, *Dynamische und kinetostatische Analyse eines räumlichen Getriebes unter Verwendung von Ersatzmassen*, PhD thesis, TU Braunschweig, Germany, 1972.
- [17] B. A. Hockey, *The Method of Dynamically Similar Systems Applied to the Distribution of Mass in Spatial Mechanisms*, Jl. of Mechanisms, pp. 169-180, 1970.
- [18] D. Pislă, N. Plitea, B. Gherman, A. Pislă, C. Vaida, "Kinematical Analysis and Design of a New Surgical Parallel Robot", Computational Kinematics. Springer, pp. 273-282, 2009.
- [19] A. Stoica, D. Pislă, "Geometric model and design of a new parallel robot used in minimally invasive surgery", Acta Technica Napocensis, pp. 503-508, 2012.
- [20] THK, General Catalogue for Linear Motion Systems, 2011.

MODELUL DINAMIC INVERS AL UNUI NOU ROBOT PARALEL FOLOSIT ÎN CHIRURGIA MINIM INVAZIVĂ

Abstract: Datorită unor intervenții chirurgicale asistate robotic, chirurgii pot opera prin incizii foarte mici, rezultând unele beneficii pentru pacienți, cum ar fi: traumatisme mai puține, pierderea de sânge redusă, timpul de recuperare mai scurt, iar pentru chirurghi reducerea tremurului mâinii, vizualizare 3D și scalarea spațiu de lucru. În lucrare este prezentat modelul dinamic invers, determinat folosind principiul lucrului mecanic virtual, al unei noi arhitecturi paralele, cât și rezultatele unor simulări ale deplasării punctului caracteristic pe o traiectorie liniară în spațiul de lucru.

Alin Stoica, Phd. Student, Departament of Mechanical Systems Engineering, Technical University of Cluj-Napoca, stoicalin1985@yahoo.com, 0264401684, Memorandumului 28, RO-400114

Bogdan Gherman, Asist. Dr. Ing., Departament of Mechanical Systems Engineering, Technical University of Cluj-Napoca, bogdangherman@yahoo.com, 0264401684, Memorandumului 28, RO-400114

Calin Vaida, S.L. Dr. Ing., Departament of Mechanical System Engineering, Technical University of Cluj-Napoca, vaida_calin@yahoo.com, 0264401684, Memorandumului 28, RO-400114

Doina Liana Pislă, -Corresponding Author- Prof. Dr. Ing., Technical University of Cluj-Napoca, Department of Mechanical System Engineering, doinapisla@yahoo.com, 0264401684, Memorandumului 28, RO-400114

Nicolae Plitea, Prof. Dr. Ing., Technical University of Cluj-Napoca, Departament of Mechanical System Engineering, nicolae.plitea@mep.utcluj.ro, 0264401684, Memorandumului 28, RO-400114